Microstructure Characterisation of Drop Tube Processed SiGe Semiconductor alloy

Naveed HUSSAIN[1] and Andrew M MULLIS[2]

[1]School of Chemical & Process Engineering, University of Leeds, Leeds LS2 9JT, UK
[2]School of Chemical & Process Engineering, University of Leeds, Leeds LS2 9JT, UK

Abstract. Si-Ge based thermoelectric materials are of interest due to the challenges associated with energy recovery from waste heat in industrial processing. A directionally solidified, chill cast ingot of $Si_{70}Ge_{30}$ was broken into pieces before being subject to rapid solidification in reduced gravity. Drop-tube processing was employed to produce a powder sample with particle diameters in the range 850-150 μm. Solidification occurred under reduced gravity conditions during free-fall down the tube. Cooling rates of between 1800 and 20000 K s^{-1} were achieved among the various particle sizes. EDX analysis was used to confirmed that the starting material, drop-tube particles and a small amount of residual material left in the crucible were all the same composition. Scanning Electron Microscopy (SEM) was used to analyse the resulting microstructure as a function of cooling rate.

The as-solidified microstructure consists of relatively large Si-rich grains with Ge localised at the boundaries, in line with the expected solidification pathway. The Ge is found to form numerous small Ge rich grains which decorate the boundaries of the much larger Si-rich grains, resulting in highly bimodal grain size distribution. This has not previously been reported in the scientific literature. The effect of cooling rate on grain size was studied using SEM and quantitative image analysis, with grain size being found, as expected, to decrease with increasing cooling rate. Point Energy Dispersive X-Ray (EDX) was conducted on all samples at areas of interest; with the larger Si rich grains showing more Si than the original alloy composition (approx. 5-15% more). The small Ge rich grains showed relatively small amounts of Si (between 3-15%). The segregation and heterogeneity found in the microstructure of rapidly solidified particles, alongside the correlation in grain sizes determined by cooling rate, would be important in understanding and improving the conversion efficiency of SiGe whilst also maximising the cost-efficiency.

Introduction

Due to their application in micro-electronics, semiconductors such as $Si_{1-x}Ge_x$ are the subject of great current interest. In particular, their tuneable band gap means that the alloy proves to be more flexible than current, pure silicon based, materials [1]. High mechanical strength and a high melting point, together with a low thermal conductivity at high temperatures (900 to 1200 K) [2], means that $Si_{1-x}Ge_x$ is often used in thermoelectrical power generation. The performance of electricity generation using heat from a thermoelectric material is determined by the dimensionless figure of merit:

$$ZT = \sigma S^2\, T/\kappa \,. \tag{1}$$

where σ is the electrical conductivity, S is the Seebeck coefficient, and κ is the thermal conductivity. The maximum efficiency is given as a function of the figure of merit ZT [3] by:

$$\eta_{max} = \frac{T_h - T_c}{T_h}\left[\frac{\sqrt{1-ZT_{ave}}-1}{\sqrt{1-ZT_{ave}}+T_c/T_h}\right]. \tag{2}$$

where T_h and T_c are the hot- and cold-side temperatures, respectively, and T_{ave} is the average $(T_h + T_c)/2$. The maximum efficiency is a product of a reduction factor along with the Carnot efficiency $(T_h - T_c)/T_h$.

Interest in SiGe alloys in industry has been due to its ability to recover power by utilising waste heat and as a result increasing cost efficiency, particularly in steel manufacturing. One of the primary challenges in developing the next generation of SiGe thermoelectric materials is to avoid altering the

characteristics of SiGe when reducing the amount of the more expensive Ge component. SiGe alloys with compositions of $Si_{92}Ge_8$ [4,5] and $Si_{95}Ge_5$ [4] using a nanostructuring approach have previously been developed, this representing a lower Ge content than the commercial alloy that is available. Electromagnetic levitation studies have found that the solidification conditions can affect the development of the microstructure, so thermal conductivity of the lower Ge content materials can be decreased by departing from thermodynamic equilibrium (i.e. increasing undercooling) [7,8,9]. In a previous study, melt spinning was used to synthesise SiGe samples and they were compared against slow cooled SiGe samples of the same composition. During close to equilibrium solidification the microstructure appeared inhomogeneous, in contrast to the rapidly solidified samples which showed a greater degree of homogeneity. Increased solute trapping was thought to be the reason behind this, with the rapidly solidified samples displaying less segregation than the sample solidified close to equilibrium. The study also found that homogeneity was improved at a higher cooling rate, alongside a decrease in grain size. [5]. Another study in 2002 compared microgravity experiments conducted on SiGe samples using the Japan Microgravity Center's (JAMIC's) drop shaft and 10m drop tube with samples processed under conventional conditions. Ground-based samples showed a higher level of segregation, though segregation was not fully suppressed even in the samples produced in microgravity. Segregation was thought to have occurred due to diffusion during unidirectional solidification [6]. Both studies found that the first region to solidify was the Si-rich grains followed by Ge-rich regions forming towards the edges and boundaries of the large distinctive Si-rich grains.

Experimental Procedure

Rapid solidification was affected by drop-tube processing. Small pieces broken from a directionally solidified, chill cast ingot of SiGe were obtained from Goodfellow. Multiple pieces of the ingot (approx. 4 g) were loaded into an alumina crucible which contained three × 300 μm laser drilled holes in the base. A graphite susceptor was used to mount the crucible at the top of the drop-tube and created a gas-tight seal to allow the molten alloy to be ejected under pressure. This was placed within a twin-walled alumina heat-shield surrounded by an induction coil that is connected to a 3 kW RF generator.

Before melting the tube is flushed three times with oxygen free nitrogen at a pressure of 40 kPa after it is evacuated to a pressure of 1 Pa using an oil-filled rotary pump. A turbomolecular pump is then used to evacuate the tube to a pressure of 10^{-4} Pa before it is filled again to 40 kPa with dried, oxygen free nitrogen gas. An R-type thermocouple within the melt crucible was used for temperature determination. A 95-minute heating cycle was employed to melt the material with an estimated 50 K superheat prior to ejection. Ejection is achieved by pressurising the crucible with 400 kPa of nitrogen gas. Further details of the drop-tube method can be found in Ref. [7]

The solidified particulate samples were collected then sieved into the following standard sieve sizes: 850 μm < d, 500 μm < d < 850 μm, 300 μm < d < 500 μm, 212 μm < d < 300 μm and 150 μm < d < 212 μm, with d being the particle diameter. Cooling rates for particles in free-fall were estimated from the balance of heat fluxes, following the method given in [7]. For particles of 850, 500, 300, 212 and 150 μm in diameter the estimated cooling rates for the undercooled liquid were 1800, 3600, 7200, 12000 and 20000 K s^{-1} respectively. Some SiGe melt remained in the crucible following the pressurisation, possibly due to the base of the crucible not being perfectly flat. The residue, starting material and drop-tube particles were all confirmed to be the same composition using EDS (described below).

In preparation for Scanning electron microscopy (SEM) the samples were mounted in TransOptic™ resin before being ground and polished. The samples were then sputter coated using a layer or Carbon. Full details of sample preparation for SEM analysis can be found in Ref [8]. The high-resolution settings in backscattered detection mode on the Hitachi SU8230 microscope were 5 kV accelerating voltage ($Vacc$) and 30 μA probe current (Ie). Grain size distribution from the SEM backscattered micrographs was analysed using the ImageJ software [9]. Electron Dispersive X-Ray (EDX) Spectroscopy maps were obtained for each sieved sample sizes, crucible residue and starting material, with point measurements also taken at areas within the micrographs of interest.

A Scheil calculation was also conducted for Si-Ge with a starting composition of 25 at. % Ge where diffusivity was assumed to be 0 in the solid fraction and infinite in the liquid. This was conducted using the CALPHAD modelling software package MTDATA [10] with version 4.3 of the SGTE database.

Results

SEM Microstructure Characterisation. A section of the starting crushed ingot was analysed using SEM backscatter to compare with rapidly solidified samples. The SEM micrograph, seen in Fig. 1a, appears to display a heterogenous microstructure with significant variations in Ge content. The microstructure of the residual crucible sample is displayed as an SEM backscatter micrograph in Fig. 1b and it also shows a heterogenous microstructure with significant variations in Ge content.

The SEM backscatter micrographs shown in Figs. 2a – 2e are associated with the drop tube processed samples of each size fraction. In contrast to previous studies we find, somewhat surprisingly, that the rapidly solidified samples show greater inhomogeneity with more visible segregation compared to either the starting or residual materials. Ge is found to be localising at the boundaries of the relatively large Si rich grains. Further investigation finds the Ge on the boundary of the large Si grains to be formed as smaller grains resulting in a bimodal grain size distribution. The segregation and Ge localisations are in line with the findings of Zhang et al [5] and Nagai et al [6], but the bimodal distribution of Si-rich grains and Ge-rich grains was not reported. Also visible are several 'cross' shapes, possibly a result of coring, within the Si grains which suggest the early signs of dendrite formation.

The results of grain size distribution analysis, for the rapidly solidified samples, can be seen in Table 1. The average grain area, in μm^2, for the Si-rich grains, Ge-rich grains and overall average grain area was investigated using a number (N) of scans at different sites within the sample(s) and this has been expressed with standard error. The average grain area can be seen to decrease as the cooling rate increases with a smaller particle size fraction.

Table 1. Average area, in μm^2, of A) Si-rich grains, B) Ge-rich grains and C) Overall average grain area observed in N number of SEM backscatter micrographs.

Grain size distribution		Average grain area in [μm^2] (and standard error)		
		Si-rich grains	Ge-rich grains	Overall average
850 μm < d	N=3	844.57 (93.73)	60.74 (6.95)	264.04 (13.54)
500 μm < d < 850 μm	N=4	812.02 (229.61)	40 (3.39)	192.26 (20.97)
300 μm < d < 500 μm	N=3	679.4 (10.22)	24.0 (0.72)	132.81 (4.87)
212 μm < d < 300 μm	N=4	467.31 (70.62)	17.51 (0.35)	102.47 (3.84)
150 μm < d < 212 μm	N=3	321.81 (30.79)	9.75 (0.65)	65.21 (2.44)

EDS Point Measurements. EDS area mapping confirmed that all samples showed the same bulk elemental composition (± 2 wt. %). EDS point measurements were taken for all samples at regions of maximum Si concentration and maximum Ge concentration and the results can be seen in figures 1 and 2 as wt. % of Si/Ge. The EDS point measurements confirm the higher level of segregation seen in the micrographs of the rapidly solidified samples as the Si-rich grains appear to have a higher Si content that the starting alloy, and Ge-rich grains consistently have over 70% Ge. A high diffusive flux resulting from strong segregation would also help explain the visible dendrite fragments at the centre of some grains.
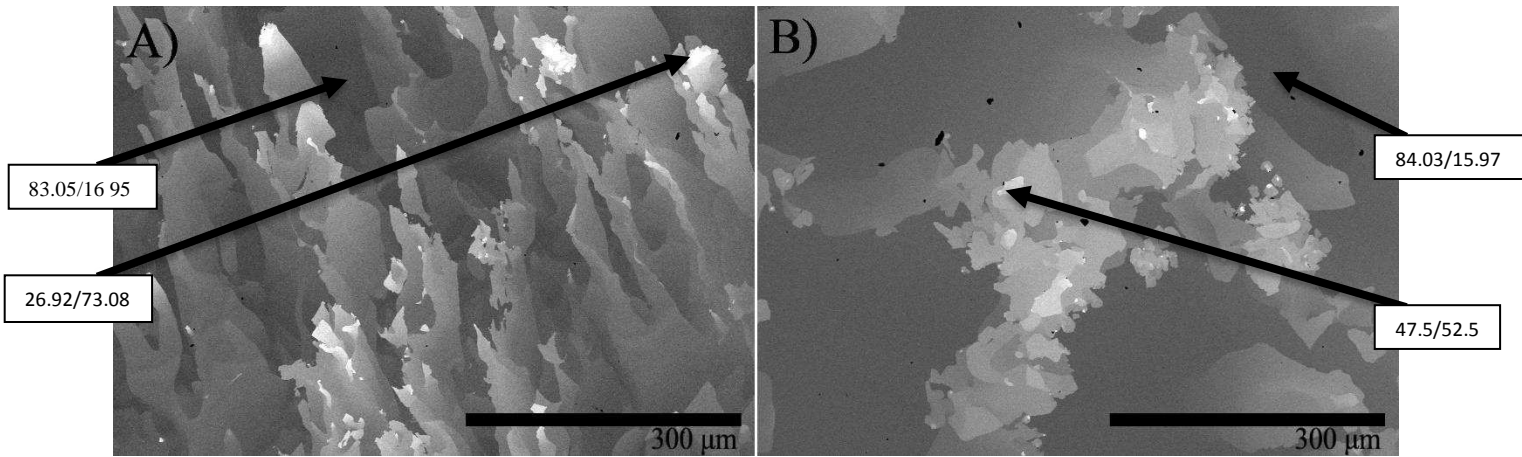
Figure 1. SEM backscatter micrographs with EDS point measurements of A) Starting ingot, and B) Crucible residue.
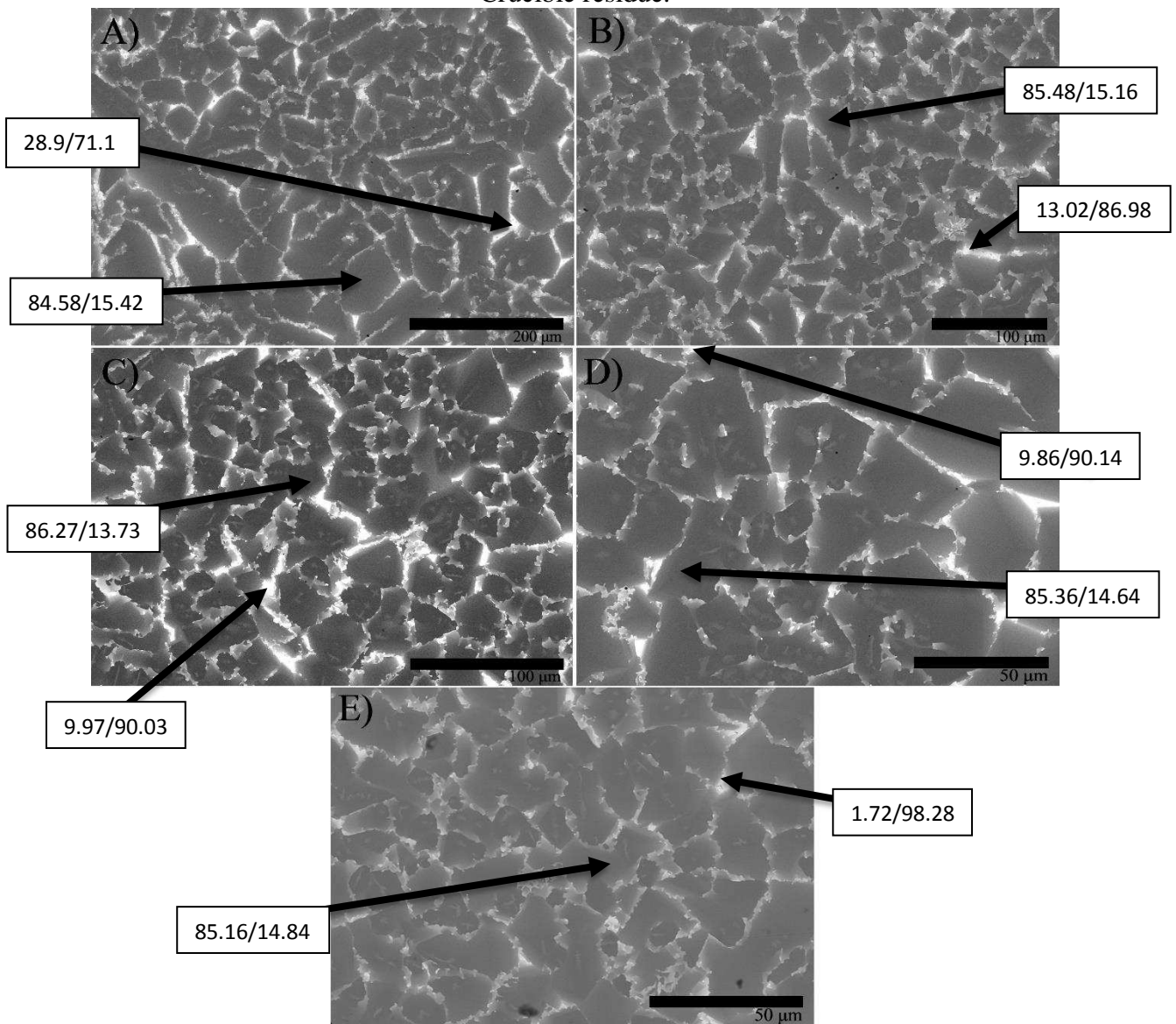

Figure 2. SEM backscatter micrographs with EDS point measurements of rapidly solidified samples with particle size fractions of A) 850 μm < d, B) 500 μm < d < 850 μm, C) 300 μm < d < 500 μm, D) 212 μm < d < 300 μm and E) 150 μm < d < 212 μm.

CALPHAD Modelling. Fig. 3 shows both the solid fraction (red) and the elemental composition of the growing solid (blue) as a function of solid fraction based upon a Scheil calculation. Noticeably, the solid fraction is seen to be strongly non-linear in the melting interval. The first solid formed is very Si-rich containing 84.3 wt. % Si and 14.7 wt. % Ge. Ge-rich regions are expected to solidify relatively late in the solidification sequence which is consistent with large Si-rich grains surrounded by grain boundaries high enriched in Ge, as observed in Fig. 2. Indeed, last parts of the microstructure to form would be expected to contain the highest concentration of Ge (approaching 100% Ge concentration).
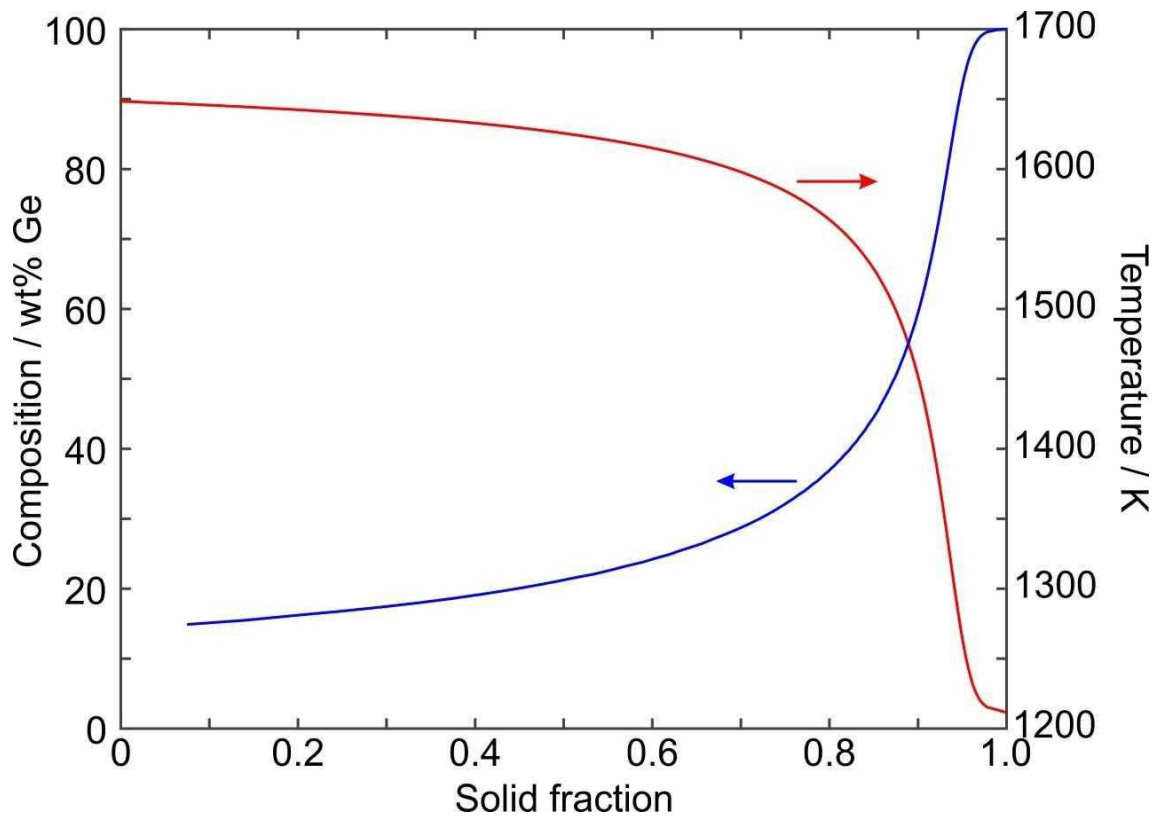

Figure 3. Scheil solidification sequence of the growing solid fraction and Ge composition in the growing solid fraction during rapid solidification.

Conclusion

It was found that the average grain size within the microstructure(s) correlated with the cooling rate, as a higher cooling rate resulted in a smaller average grain size. Both the microstructures found in SEM micrographs and the EDS point measurements seem to agree with the Scheil calculation with large Si grains expected to form first, and the solid fraction of the highest concentration of Ge to form at the end of solidification and occupy the Si grain boundaries. EDS point measurements also showed that the level of segregation found was higher than previously reported.

The formation of a bimodal distribution with Si-rich grains followed by Ge-rich grains was found in the SEM backscatter images but interestingly this was not previously reported despite a similar microstructure found by Zhang et al [5] and Nagai et al [6].

References

[1] R. R. King, N. H. Karam and M. Haddad, "Multijunction photovoltaic cells and panels using a silicon or silicon-germanium active substrate cell for space and terrestrial applications.". US Patent US 6340788 B1, 2002.

[2] C. B. Vining, "Thermoelectric Properties of Silicides," in CRC Handbook of Thermoelectrics, 1 ed., N. Sullivan, Ed., CRC Press LLC, 1995, pp. 329-337.

[3] A. F. Loffe, Physics of semiconductors, New York: Academic Press Inc., 1960.

[4] G. Bernard-Granger, K. Favier, M. Soulier, C. Navone, M. Boidot, B. Deniau, P. Grondin, J. Leforestier and J. Simon, "Thermoelectric properties of an N-type silicon–germanium alloy related to the presence of silica nodules dispersed in the microstructure.," Scripta Materialia, vol. 93, p. 40–43, 2014.

[5] G. H. Zhu, H. Lee, Y. C. Lan, X. W. Wang, G. Joshi, Z. W. Wang, J. Yang, D. Vashaee, H. Guilbert, A. Pillitteri, M. S. Dresselhaus, G. Chen and Z. F. Ren, "Increased Phonon Scattering by Nanograins and Point Defects in Nanostructured Silicon with a Low Concentration of Germanium," Physical Review Letters, vol. 102, 2009.

[6] B. Yu, M. Zebarjadi, H. Wang, K. Lukas, H. Wang, D. Wang, C. Opeil, M. Dresselhaus, G. Chen and Z. Ren, "Enhancement of Thermoelectric Properties by Modulation-Doping in Silicon Germanium Alloy Nanocomposites.," Nano Letters, vol. 12, no. 4, p. 2077–2082, 2012.

[7] L. K. Eckler and D. M. Herlach, "Evidence for Transitions from Lateral to Continuous and to Rapid Growth in Ge-lat%Si Solid Solution.," Europhysics Letters, vol. 32, no. 3, pp. 223-227, 1995.

[8] R. P. Liu, T. Volkmann and D. M. Herlach, "Undercooling and solidification of Si by electromagnetic levitation," Acta Materialia, vol. 49, p. 439–444, 2001.

[9] C. Panofen and D. M. Herlach, "Rapid solidification of highly undercooled Si and Si–Co melts," Applied Physics Letters, vol. 88, pp. 171913-171913-3, 2006.

[10] P. Zhang, Z. Wang, H. Chen, H. Yu, L. Zhu and X. Jian, "Effect of Cooling Rate on Microstructural Homogeneity and Grain Size of n-Type Si-Ge Thermoelectric Alloy by Melt Spinning," Journal of Electronic Materials, vol. 39, no. 10, pp. 2251-2254, 2010.

[11] H. Nagai, Y. Nakata, H. Minagawa, K. Kamada, T. Tsurue, M. Sasamori and T. Okutani, "Synthesis of Si–Ge Alloy by Rapid Cooling in Short-Duration Microgravity," Japanese Journal of Applied Physics, vol. 41, pp. 749-753, 2002.

[12] O. Oloyede, T. D. Bigg, R. F. Cochrane and A. M. Mullis, "Microstructure evolution and mechanical properties of drop-tube processed, rapidly solidified grey cast iron," Materials Science & Engineering A, vol. 654, p. 143–150, 2016.

[13] N. Hussain, A. M. Mullis and J. S. Forrester, "Effect of cooling rate and chromium doping on the microstructure of Al-25 at.% Ni Raney type alloy," Journal of Alloys and Compounds, vol. 744, pp. 801-808, 2018.

[14] J. Schindelin, I. Arganda-Carreras, E. Frise, V. Kaynig, M. Longair, T. Pietzsch, S. Preibisch, C. Rueden, S. Saalfeld, B. Schmid, J.-Y. Tinevez, D. J. White, V. Hartenstein, K. Eliceiri, P. Tomancak and A. Cardona, "Fiji: an open-source platform for biological-image analysis," Nature Methods, vol. 9, p. 676–682, 2012.

[15] R. H. Davies, A. T. Dinsdale, J. A. Gisby, J. A. J. Robinson and S. M. Martin, "MTDATA - Thermodynamics and Phase Equilibrium Software from the National Physical Laboratory," CALPHAD, vol. 26, no. 2, pp. 229-271, 2002.